Current Applied Physics 11 (2011) 182–187

Contents lists available at ScienceDirect

Current Applied Physics

journal homepage: www.elsevier.com/locate/cap

Ion beam analysis of sputtered AlN films

Arshad Mahmood [a,*], E. Andrade [b], S. Muhl [c], A. Shah [a], M. Khizar [d], M. Yasin Akhtar Raja [d]

[a] National Institute of Lasers and Optronics, P. O. Nilore, Islamabad, Pakistan
[b] Instituto de Física, UNAM, Apdo. Postal 20-364, Mexico D. F., CP 0100, Mexico
[c] Instituto de Investigaciones en Materiales, UNAM, Apdo. Postal 670-360, D.F., 04510, Mexico
[d] Center for Optoelectronic and Optical Communications, University of North Carolina, Charlotte, United States

ARTICLE INFO

Article history:
Received 23 October 2009
Received in revised form
1 July 2010
Accepted 2 July 2010
Available online 13 July 2010

Keywords:
AlN
Reactive sputtering
Rutherford backscattering
AFM
Ellipsometry

ABSTRACT

Polycrystalline aluminium nitride (AlN) films have been prepared by DC reactive magnetron sputtering followed by its characterization using advance electronic and optical techniques. Film quality has been optimized mainly using deposition parameters. Rutherford backscattering spectroscopy (RBS) and nuclear interaction (NR) techniques were used to analyze the film density (atoms/cm^3), elemental composition and impurities of the grown film. Our ion beam analysis (IBA) was based on the particle energy spectra bombarded with a low-energy deuterium beam. The corresponding linear thickness of the film was measured using a profilometer. X-Ray diffraction, spectroscopic ellipsometry and atomic force microscope have also been employed to reinforce the results. We found that highly dense and stoichiometric films can be obtained at higher plasma current. Under optimal deposition conditions, the film densities of $\sim$2.45 g/cm^3, FWHM $\sim$0.125 and the surface roughness $\sim$6.758 nm have been achieved successfully.

1. Introduction

The exceptional properties of AlN make this material a promising candidate for a variety of technological applications. AlN has been widely investigated as an exceptional electronic and UV optoelectronic material [1,2] for its wide bandgap (Eg $\sim$6.2 eV) and favorable acoustic and optical properties [3,4]. In particular, it possesses high surface acoustic wave velocity, good temperature stability and a sizeable electromechanical coupling coefficient [5]. The major technological implications of producing high quality AlN thin film are its outstanding electrical, thermal and dielectric properties. Such as, these films have a large thermal conductivity of 3.9 W/(cm K) at 300 K and a small thermal expansion coefficient 6.3×10^{-6} K^{-1}. This is a hard semiconducting material with excellent corrosion and wear resistance [6–8].

AlN is easy to prepare but for device applications, good quality films like, high degree of crystalline orientation, smooth surface and precise thickness and density control, are required. Despite ongoing research work on AlN growth during the last several years, still, there is a need to control the physical properties of this material by the deposition conditions. In past, various deposition techniques e.g., chemical vapor deposition (CVD) [9], reactive sputtering [10–15], reactive evaporation [16], molecular beam epitaxy (EBM) [17,18], ion beam-assisted deposition [19], laser assisted CVD [20], plasma assisted CVD [21] and metallorganic chemical vapor deposition (MOCVD) [22] have been used. However, due to better control on the deposition parameters, reactive magnetron sputtering (RMS) technique has attended tremendous attention for several semiconductors including SiC [23] and AlN [24]. This is mainly because of their lower growth temperature capabilities. It has been reported that the lattice mismatch and other related defects can be reduced by using the low substrate temperature to produce good quality films for microelectronic applications [22,23].

During this study, we have found that the elemental composition of the AlN_x is critical to identify the corresponding film phases and also its correlation with the deposition conditions. Among other techniques, IBA may be very attractive for the analysis of composition, impurities, and density of thin films. We have exploited a DC-RMS technique to prepare a good quality AlN films. Advance characterization techniques such as IBA (ion beam analysis), XRD and AFM have been used to establish a correlation between the physical properties and the corresponding deposition parameters of the grown film. Furthermore, two techniques for ion beam analysis have also been employed to investigate the effects of the stoichiometry, density and impurities on the over all quality of the film.

* Corresponding author. Tel.: +92 51 929 0231/3206; fax: +92 51 929 0275.
E-mail addresses: arshad_junjua@yahoo.com, drarshadjanjua@gmail.com (A. Mahmood).

1567-1739/$ – see front matter © 2010 Elsevier B.V. All rights reserved.
doi:10.1016/j.cap.2010.07.003

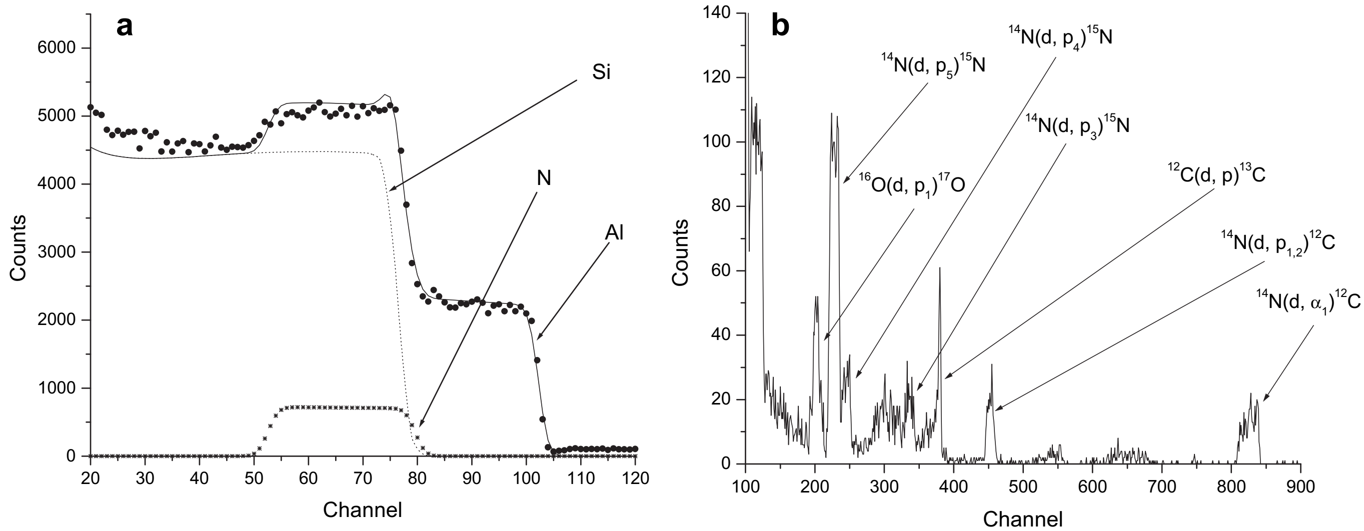

Fig. 1. a. The RBS spectrum (low-energy part) arising from elastically scattered beam particles. b. The high energy part containing the peaks from N, O and C nuclear interaction peaks.

2. Experimental setup

The films were grown in a turbo molecular pumped ultrahigh vacuum reactive magnetron sputtering system with a base pressure of 3×10^{-7} Torr. The system was equipped with a 4-inch magnetron source and the used target material was a high purity (99.999%) electronic grade aluminium disc, which was clamped against the water-cooled cathode surface. Sputtering was carried out in mixed Ar–N_2 discharges at different plasma currents. The purity of Ar and N_2 gases was 99.999%. For this work, the pressure, total gas flow and target to substrate distance were kept constant at 6 mTorr, 10 sccm and 3 cm, respectively. The substrates were pieces of Si (100) which were chemically cleaned prior to the insertion in the vacuum chamber.

A 1050 keV $^2H^+$ beam was selected as the IBA method for the characterization of the AlN_x films. A 300 μm thick surface barrier detector set at $\theta = 150°$ with a solid angle $\Omega = 4$ msr was used to measure the energy of the particles produced by the ion bombardment perpendicular to the surface of the film. The energy resolution was about 20 keV at FWHM. We did not use particle absorbing foil in front of the detector in order to detect both the particles produced elastically (RBS) and by nuclear interaction. As a trade-off for not using two detectors (the RBS and the NR detector with a absorbing foil) method, we have to use low beam current ($\approx$5 nA) in order to avoid pile up pulses in the particle energy spectra. Using one detector, the parameters $\Omega.N.$ (total beam particles $\times$ msr) needed in the NR analysis, can be obtained from the RBS spectrum analysis.

The IBA facilities of the Institute of Physics of the National Autonomous University of Mexico based on a 5.5 MV CN Van de Graaff accelerator [24] was used to obtain the atomic composition of the AlN_x films and the atomic areal density. Several possibilities were considered to choose appropriate IBA methods to analyze the films. It is known that a standard Rutherford backscattering

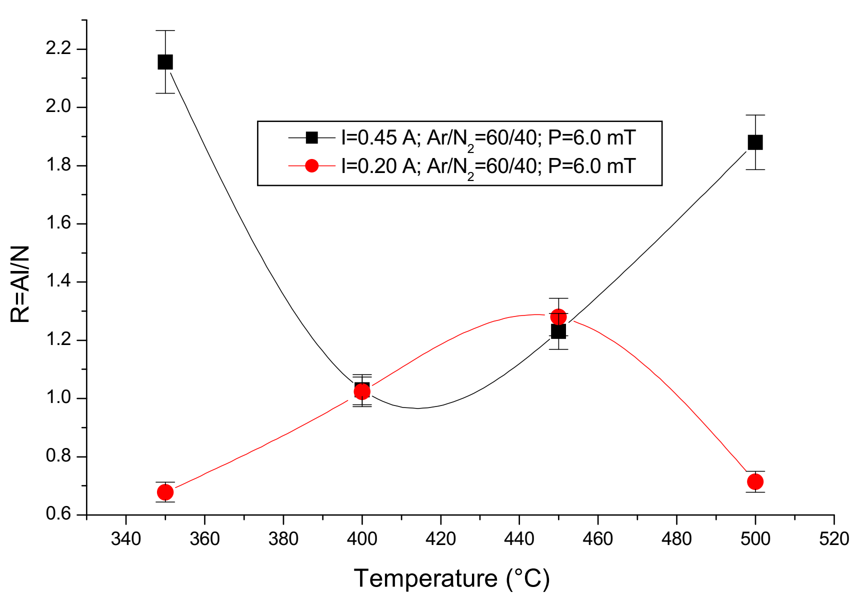

Fig. 2. The variation of elemental composition Al/N with substrate temperature for (a) $I = 0.45$ A and (b) $I = 0.2$ A, $T_s = 400$ °C, Ar/N_2 = 60/40 and $P = 6.0$ mT.

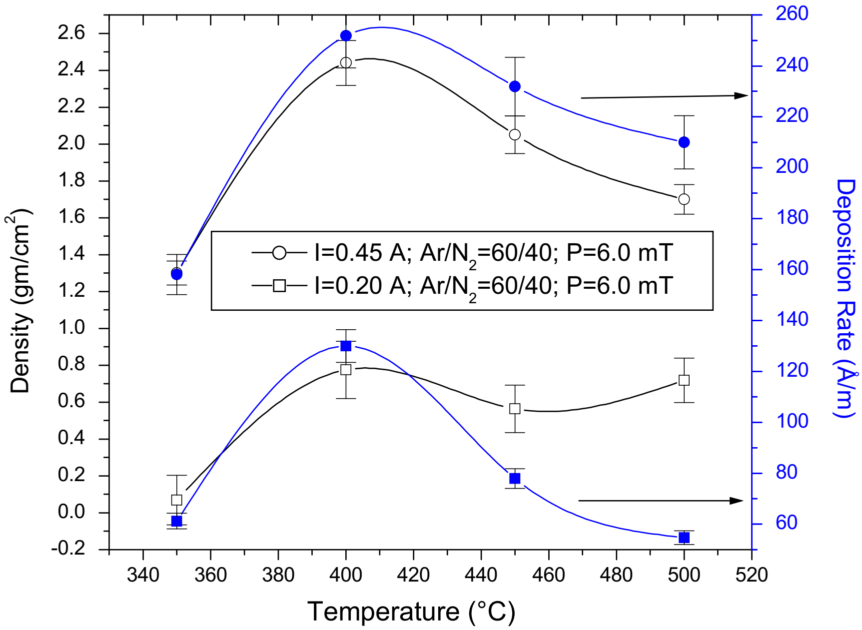

Fig. 3. The variation of (a) deposition rate versus substrate temperature and (b) the density versus temperature for films prepared using $Ar/N_2 = 60/40$, $I = 0.45$ A and $I = 0.2$ A.

spectroscopy is best used to profile the distribution of heavy elements in matrices composed of light elements. Nuclear interaction analysis (NIA) for positive "Q" values such as: (d, p), (d, α), is ideal for profiling the elemental distribution of medium light elements (like O, N, C, etc.) on heavier substrate where the RBS is particularly insensitive. ^{2}H ions induce high Q nuclear interactions on N, O, C (e.g.: ^{14}N (^{2}H, α_0) ^{12}C/Q = 13,574 keV, ^{14}N (^{2}H, α_1) ^{12}C/Q = 9146 keV, ^{14}N (^{2}H, p_0) ^{15}N/Q = 8610 keV, ^{16}O (^{2}H, α_0) ^{14}N/Q = 3110 keV, ^{12}C (^{2}H, p_0) ^{12}C/Q = 2722 keV.

The composition profile of the samples was obtained by simulating the particle energy spectra using the SIMNRA program [25]. This program can be used to analyze the RBS and NR regions of each particle spectra. The detection geometry $\theta = 150°$ has been chosen because nitrogen NR cross-section has been used to obtain the nitrogen profile concentrations of the AlN_x films. Also other, experimental cross-sections can be introduced to this software using the R33 format [24].

For the surface morphology analysis of the prepared film, a nanoscope-A of Digital Instruments has been used. The linear film thickness "*t*" (μm) was measured using a Salon Desktak IIA profilometer. Graphite or silicon strips of about 1 mm wide were used to mask the edge of films substrate. These strips help provide necessary step height between the edge of the deposit and the substrate.

3. Experimental results

A typical energy spectrum (dots) of a 1140 keV ^{2}H ions incident at angle 0° with respect to the normal on the AlN_x film deposited on

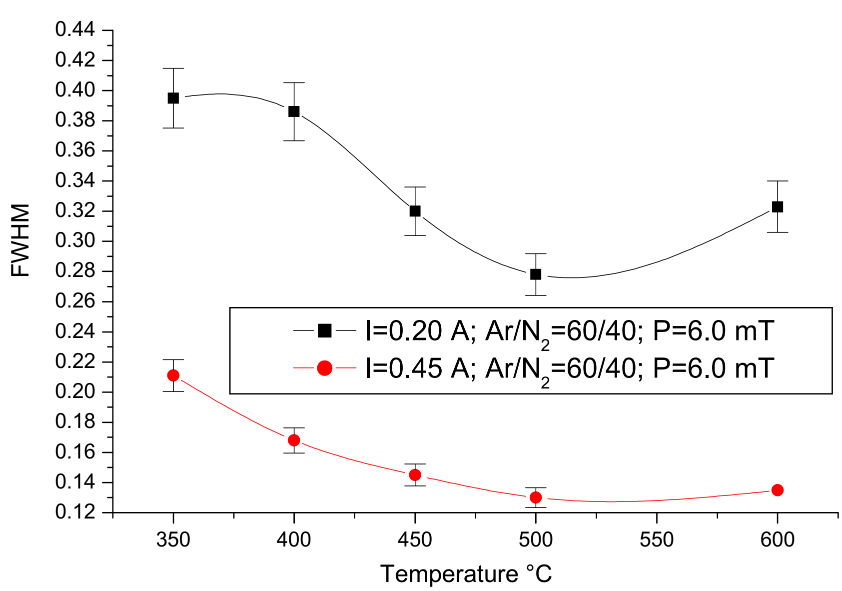

Fig. 4. The variation of FWHM with the gas composition for $T = 400$ °C, $P = 6.0$ mT and (a) $I = 0.2$ A and (b) $I = 0.45$ A.

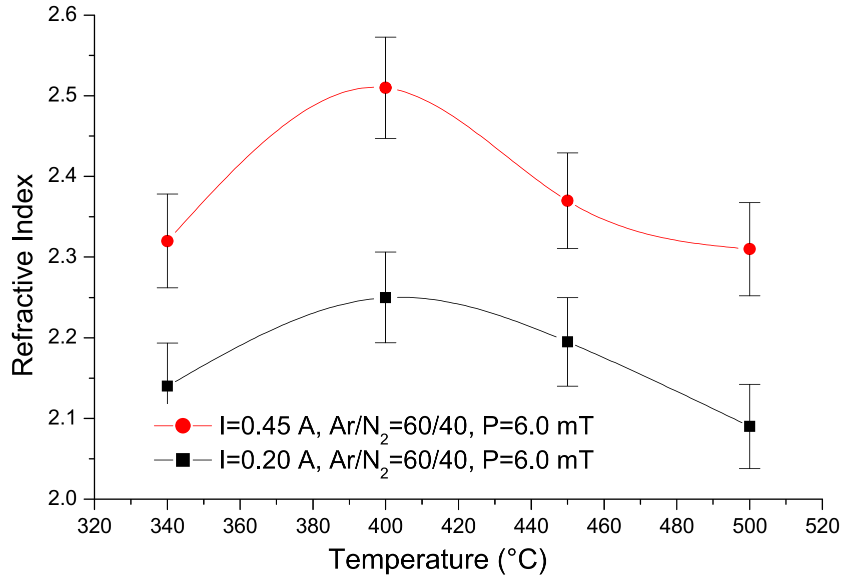

Fig. 5. The variation of refractive index with substrate temperature for the deposition conditions $Ar/N_2 = 60/40$, $I = 0.45$ A and $I = 0.2$ A.

a c-Si substrate is shown in Fig. 1(a, b). Fig. 1(a) shows the low-energy portion of the spectra arising from elastically scattered beam particles, whereas, the high energy part containing the peaks from N, O and C nuclear interactions is depicted in (b). The quantitative analysis of the spectrum (solid line) was made by simulating the spectrum using the SIMNRA program [25]. It has been found that this particular computer code is more versatile compared to its counterpart RUMP program. Primarily, this is because SIMNRA code includes the N, C and O NR cross-sections, non-Rutherford cross-sections and multiple and plural scattering.

The low and high energy part of the spectrum has been simulated with the set of parameter described with Fig. 1. Based on experimental data by IBA, we successfully obtained the atomic areal density and the percentage of composition of Al, N, O and C of the films. We found that the oxygen in the films is due to the oxidation of the AlN. Part of the carbon concentration may be due to atmospheric contamination and carbon beam build up.

In brief, the most important nuclear interaction (NR) with positive "Q" values is the following: $^{14}N(d,\alpha_1)^{12}C^*$, $^{14}N(d, p_i)^{15}N^*$ [$i = 1, 2, 3, 4, 5$ and 6], $^{16}O(d,p_1)^{17}O$, $^{16}O(d,p_2)^{17}O$,$^{16}O(d,\alpha_0)^{14}N$ and $^{12}C(d,p_0)^{13}C$. This NR may be observed as peaks in the high energy part of the particle energy spectrum with almost free background counts. The knowledge of the NR cross-sections and the area peaks can be used to deduce the N, O and C concentration profiles in the bombarded samples. In order to use only one solid state detector, no absorbing foil was used in front of the detector. This technique has been very effective to measure the elastically backscattered beam particle and all the NR particles. Further, a low beam ~10 nA was used to avoid counts pile up in the energy particle spectra.

Fig. 2 demonstrates the variation of elemental composition Al/N with temperature for (a) $I = 0.45$ A and (b) $I = 0.2$ A, $T_s = 400$ °C, $Ar/N_2 = 60/40$ and $P = 6.0$ mT. It is interesting to note that the stoichiometric deposits may be produced at lower nitrogen concentration at both sets of plasma current. Temperature also plays an important role to prepare stoichiometric AlN films. Moreover, for the case of higher current, Al content is higher ($Al/N > 1$) while it is lower for low plasma current ($Al/N < 1$).

The variation of (a) deposition rate versus temperature and (b) the density versus temperature for films prepared using $Ar/N_2 = 60/40$, $I = 0.45$ A and $I = 0.2$ A are demonstrated in Fig. 3. Based on the results obtained by Fig. 3, it is attributed that there is a direct relation between the density of the deposit and the deposition rate. It is interested to note that the film density is divided clearly into two sets. The deposits present the lower density trend for lower plasma current ($I = 0.2$ A), whereas, the density is significantly higher for higher plasma current ($I = 0.45$ A) at all deposition conditions.

The variation of FWHM with the gas composition for $T = 400$ °C, $P = 6.0$ mT and (a) $I = 0.2$ A and (b) $I = 0.45$ A has been shown in Fig. 4. It is observed that lower values of FWHM can be obtained when the nitrogen concentration is lower in the mixture of gases. This figure also demonstrates the behaviour of the variation of the FWHM at lower and at higher plasma powers. It is observed that at higher plasma current, FWHM has lower trend at all values of gas composition. The variation of refractive index with temperature is depicted in Fig. 5 at plasma current $I = 0.2$ A and 0.45 A. This demonstrates that the refractive index is higher at all temperatures for the corresponding higher plasma current.

Fig. 6 (a–c) shows the 3D surface morphology AFM images of the film. Moreover, the roughness and grain size have also been calculated. It is observed that the roughness can be decreased up to 6.578 nm while the grain size of 34.34 nm can be obtained for plasma current $I = 0.45$ A, $Ar/N_2 = 60/40$ and $T = 400$ °C, $P = 6.0$ mT.

4. Discussion

The IBA results obtained dictate that the presence of oxygen in the film is due to the oxidation of film surface for high electron affinity of Al. Carbon found on the surface of the film is primarily due to atmospheric contamination, however, no Ar signatures were observed during this analysis.

We found that the optimized deposition conditions like higher plasma power and lower nitrogen concentration are key to prepare good quality films. The factors, which determine the quality of the film, are generally, high crystalline alignment (i.e. lower values of FWHM), high density and larger and fine grain structure, which have strong influence to improve the over all physical properties of the film. The dependency of the reactive magnetron sputtered film quality on the deposition parameters has also been studied. We also found that the possible film formation process plays an important role to improve the film properties, that may have a direct

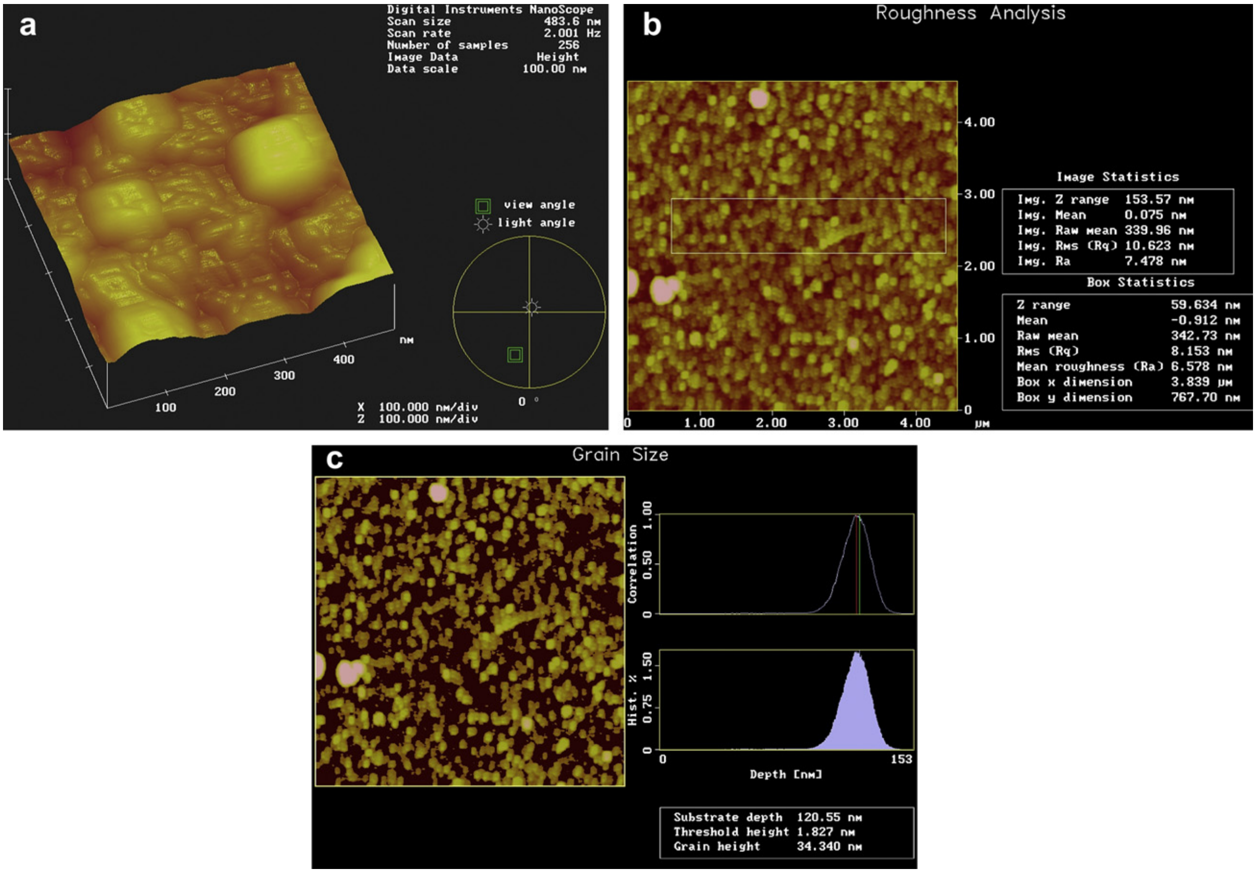

Fig. 6. The AFM images, (a) morphology, (b) roughness and (c) grain size of the film prepared for plasma current, $I = 0.45$ A, $Ar/N_2 = 60/40$ and $T = 400$ °C, $P = 6.0$ mT.

correlation with the deposition conditions. Most of the results presented above can be attributed based on the following processes:

When an Al target is to be sputtered in a mixture of reactive gases, the most densely packed films with high crystallinity can be formed. But, again the experimental conditions play an important role whether the compound is formed on the target surface or the reaction took place on the substrate.

1. When the plasma current is lower and the N_2 concentration is higher in plasma ($N_2/Ar > 1$), AlN compound is formed by a bombardment assisted chemical reaction on the surface of the Al target, that may be sputtered and condense directly on the substrate forming AlN films. In this case, we have observed preferential orientation of crystallites in our samples but the film property is lower, meaning FWHM is high and density and grain size are lower.
2. When plasma current is lower under the limited supply of N_2 concentration ($N_2/Ar < 1$), the sputtering rate is to be increased due to the abundant supply of heavy Ar atoms. Here, the formation of AlN is again done mostly on the target surface but there is also a possibility that the arrival rate of plasma-generated particles on the substrate is increased due to increased sputtering rate. The single oriented films in the 0002 direction (AlN presents piezoelectric property in the 0002 direction) are obtained. The films are almost stoichiometric but still show somewhat lower density and higher FWHM.
3. On the other hand, when plasma current is to be increased under low N_2 concentration ($N_2/Ar < 1$), the sputtering of Al target becomes more efficient and high energy N_2^+ radicals along with N_2^* metastable radicals are also produced within the sputtering plasma.

This indicates that when the reactive radicals got higher energy in appropriate composition, the reaction on the substrate and also on the surface of the target is enhanced to improve the quality of the film. The highly polycrystalline single oriented films with high density and lower value of FWHM have been produced at higher plasma current. Harper et al. [26] have also showed that the preferred orientation along c-axis can be obtained with $E(N_2^+) =$ 100–200 eV, while the c-axis changed in the plane of the film for $E(N_2^+) > 400$ eV. The same observation was reported by Windschmann et al. [19]. We have found that the plasma density and electron temperature generally increases as the plasma power increases, although changes in the gas composition can also be of importance. Moreover, the increase in the deposition rate would have to be accompanied by a significant change in the Al/N ratio as the plasma power is increased.

5. Conclusion

In order to obtain good quality AlN films with highly crystalline and good optical, mechanical and structural properties, an ion beam analysis technique has been employed to study the effects of elemental composition, density and impurities present in the film. The role of ion bombardment in film formation by plasma current and substrate temperature during DC sputtering, has been observed in order to control the grain size, surface morphology, and density of AlN films.

It is found that the lower nitrogen concentration and higher plasma current and substrate temperature are key to obtain pure AlN films with high density and lower concentration of impurities in the film. Moreover, it is observed that by using optimum deposition conditions, highly epitaxial crystalline films with lower FWHM and high refractive index can be produced. Whereas, the optical properties can be related with the crystalline alignment and density of the film.

References

[1] P.M. Lundquist, W.P. Lin, Z.Y. Xu, et al., Appl. Phys. Lett. 65 (1994) 1085.
[2] D. Brunner, H. Angerer, E. Bustarret, F. Fuedenberg, R. Hopler, R. Dimitrov, O. Ambacher, J. Stutzmann, Appl. Phys. 82 (1997) 5090.
[3] M.B. Assouar, O. Elmazria, L. Le Brizoual, P. Alnot, Diamond Relat. Mater. 11 (2002) 413–417.
[4] R.F. Davis, Proc. IEEE 79 (1991) 702.
[5] K. Tsubouchib, K. Sagai, Micishiba, Proc. IEEE Symp. Ultrason 14 (1983) 340.
[6] E.I. Meletis, S. Yan, J. Vac. Sci. Technol. A 9 (1991) 2279.
[7] T.J. Meroz Jr., Ceram. Bull. 71 (1992) 782.
[8] David M. Teter, MRS Bulletin (Jan 1998) 22.
[9] J.L. Dupuie, E. Gulari, J. Vac. Sci. Technol. A 10 (1992) 18.
[10] T. Shiosaki, T. Yamamoto, T. Oda, A. Kawabata, Appl. Phys. Lett. 36 (1980) 643.
[11] E. Valcheva, J. Birch, P.O.A. Persson, S. Tungasmita, L. Hultman, J. Appl. Phys. 100 (2006) 123514.
[12] J.X. Zhang, H. Cheng, Y.Z. Chen, A. Uddin, Shu Yuan, S.J. Geng, S. Zhang, Surf. Coat. Technol. 198 (2005) 68–73.
[13] Hong-Ying Chen, Sheng Han, Han C. Shih, Surf. Coat. Technol. 200 (2006) 3326–3329.
[14] V. Brien, P. Pigeat, J. Cryst. Growth 299 (2007) 189–194.
[15] C.K. Lee, S. Cochran, A. Abrar, K.J. Kirk, F. Placido, Ultrasonics 42 (2004) 485–490.
[16] R. Bensalem, A. Abid, B.J. Selly, Thin Solid Films 143 (1986) 141.
[17] H.-U. Baier, W. Moench, Appl. Surf. Sci. 56–58 (1992) 766.
[18] Z. Sitar, L.L. Smith, R.F. Davis, J. Cryst. Growth 141 (1994) 11.
[19] H. Windischmann, Thin Solid Films 154 (1987) 159.
[20] X. Li, T.L. Tansley, J. Appl. Phys. 68 (1990) 5369.
[21] W. Zhang, Y. Someno, M. Sasaki, T. Hirai, J. Cryst. Growth 130 (1993) 308.
[22] C.R. Aardahl, J.W. Rogers Jr., H.K. Yun, Y. Ono, D.C. Tweet, S.-T. Hsu, Thin Solid Films 346 (1999) 174.
[23] Q. Wahab, L. Hultman, J.E. Sundgren, M. Willander, J. Mater. Sci. Eng. B 11 (1992) 61.
[24] E. Andrade, Nucl. Instrum. Methods Phys. Res. B 56/57 (1991) 802.
[25] L.R. Doolittle, Nucl. Inst. Math. Phys. Res. B 15 (1986) 227.
[26] J.M.E. Harper, J.J. Cuomo, H.T.G. Hentzell, Appl. Phys. Lett. 43 (1983) 547.